# Loop I Can Modulate ADP Affinity, ATPase Activity, and Motility of Different Scallop Myosins. Transient Kinetic Analysis of S1 Isoforms†

S. E. Kurzawa-Goertz,‡ C. L. Perreault-Micale,§,⊥ K. M. Trybus,|| A. G. Szent-Györgyi,⊥ and M. A. Geeves*,‡

*Max-Planck-Institut für Molekulare Physiologie, Dortmund 44139, Germany, and Department of Biology and Rosenstiel Basic Medical Sciences Research Center, Brandeis University, Waltham, Massachusetts 02254-9110*

*Received November 19, 1997; Revised Manuscript Received February 3, 1998*

ABSTRACT: The striated muscle myosin of *Placopecten* moves actin faster in in vitro motility assays and has a higher actin-activated ATPase turnover rate than the myosin of the catch muscle. The heavy chain sequences of the two PlacoS1s are almost identical except at the surface loop 1 near the nucleotide binding pocket, where the two sequences vary significantly. *Argopecten* striated muscle myosin is 96% identical to *Placopecten* striated myosin, and both move actin with a similar velocity. To identify the individual kinetic steps which differ between these myosins, we completed a transient kinetic characterization of the three myosin S1s. The two striated S1s have similar rates of nucleotide binding to S1 and to acto·S1. The largest differences between the two are in the rate of ADP dissociation from S1 and affinity of ADP to S1, which differ by a factor of 2. The rates of nucleotide binding, nucleotide dissociation and affinity to nucleotides of the two *Placopecten* S1s are similar and agree within a factor of 2. In contrast, the affinity of acto·S1 for ADP is nine times weaker for the striated acto·S1 than for the catch acto·S1, compatible with the differences in motility of the *Placopecten* myosins. Thus the differences in ADP affinity to acto·S1 and in the in vitro motility can be attributed to the differences in surface loop 1.

Molluscan catch muscles are unique in that they can maintain tension at the expense of a very low metabolic turnover rate. The muscles are stiff in the catch state so that tension is retained, although contractile processes are inhibited. In addition to these tonic slow muscles, molluscs contain faster phasic muscles. The catch muscles enable the organism to keep its shell closed for long periods by compressing the elastic ligament at the hinge, while the faster phasic muscles have properties similar to those of vertebrates. In scallops the phasic muscles are striated, while the catch muscles are smooth and contain large amounts of paramyosin. It is thought that tension can be maintained by the very slow cycling of the myosin cross-bridges, although the contribution of paramyosin to the catch state cannot be excluded. To regulate the catch state, these muscles require additional regulatory controls. Phosphorylation has been considered to specifically regulate catch contraction. The catch state is interrupted by cAMP in skinned fibers of the byssus retractor muscles of *Mytilus edulis* (*1*). Phosphorylation of the myosin heavy chains (*2*), the regulatory light chains (*3*), and paramyosin (*4*, *5*) has been demonstrated (*6*). Nevertheless, it is unclear how these phosphorylations relate to the catch state.

Catch muscle myosins have a considerably lower steady-state ATPase activity than myosins of phasic muscles. The actin-activated Mg-ATPase of myosin from the striated adductor muscle of the sea scallop, *Placopecten magellanicus*, is severalfold greater than that of the myosin from its smooth adductor muscle. Similarly, the ATPase activity of the striated *Placopecten* muscle myosin exceeds significantly the activity of the striated adductor myosin of the bay scallop, *Argopecten irradians* (*7*, *8*). The shortening speed of many muscles is correlated with the ATPase activity of actomyosin (*9*) or with the ADP release rate (*10*). However, these functions can be uncoupled, as shown by in vitro motility assays. The importance of the surface loops in modulating ATPase activities and motility has been recently pointed out by Spudich (*11*). The two flexible surface loops are poorly conserved in sequence and in composition among different myosins and are, therefore, most likely candidates to modulate ATPase activities and the velocity of movement in motility assays. The two surface loops may act independently. Substitutions of surface loop 2 (50/20-kDa junction) to produce chimeric *Dictyostelium* myosins showed that the $V_{max}$ of the actin-activated ATPase correlated with the parent myosin from which the sequence was derived, while velocity of movement was only little affected (*12*). To explain the discrepancy between motility and ATPase activity, it was proposed that surface loop 2 regulated $V_{max}$ of the ATPase while surface loop 1 modulated motility by altering ADP release rates (*11*). Recent studies with partially digested rabbit myosin indicated that loop 1 can modulate motility without affecting ATPase activity, in support of this model (*13*). However, a number of studies indicate that surface loop 1 can alter ATPase activities as well (*7*, *14*−*16*).

† This work was supported by the Max-Planck Society (M.A.G.), NIH Grants HL3813 (K.M.T.) and AR15963 (A.G.S.), and a grant from the Muscular Dystrophy Association (A.G.S.).

* Corresponding author.

‡ Max-Planck-Institut für Molekulare Physiologie.

§ Present address: Cardiovascular Division, Beth Israel Deaconess Medical Center, Boston, Massachusetts 02254.

⊥ Department of Biology, Brandeis University.

|| Rosenstiel Basic Medical Sciences Research Center, Brandeis University.

S0006-2960(97)02844-4 CCC: $15.00 
Published on Web 04/28/1998

Scallop muscles are particularly useful to determine the steps in the ATPase cycle that are modulated by loop 1. The myosins of catch and striated adductors arise from the alternative RNA splicing of a single myosin heavy chain gene both in *Placopecten* (*7*) and in *Argopecten* (*17*). The putative amino acid sequences between the heavy chains of the isoforms of the same species are well conserved with an identity of 97%. The identity between the two striated and catch myosin heavy chains is also very high. The differences in ATPase activities are also present in the unregulated subfragment-1 (S1)[1] preparations and are not due to light chains. The sequences of the *Placopecten* striated and catch myosin heavy chain motor domains diverge only in the flexible surface loop near the nucleotide binding pocket and in a small segment encoded by exon 13. The major change between the two heavy chains of the striated myosins is in a 10-residue portion of the same flexible loop which is changed in the catch muscle and a series of conservative point mutations throughout the head. This indicates that this flexible loop at the 25/50-kDa junction modulates ATPase activities in molluscan muscles (*7*). In this study we have employed transient kinetics to focus on the step that controls the different ATPase rates. We show that the *Placopecten* catch acto·S1 preparations bind ADP with a higher affinity than striated acto·S1s. We also find that the rate of movement of the myosins parallels ATPase activity.

## EXPERIMENTAL PROCEDURES

*Proteins and Reagents.* Rabbit actin was purified by the method of Lehrer and Kerwar (*18*) and labeled with pyrene (pyr-actin) as previously described (*19*). The 2'(3')-*O*-(*N*-methylanthraniloyl) derivatives of ATP and ADP (mantATP/ADP) were prepared by reaction with *N*-methylisatoic anhydride (*20*), except that after the reaction they were purified on a DEAE cellulose column (*21*).

Scallop myosins were prepared from the striated adductor muscles of *Argopecten irradians* ($Ar^{st}$) and the striated and catch adductors of *Placopecten magellanicus* ($Pl^{st}$ and $Pl^{c}$) (*22*). S1s were prepared from $Ar^{st}$ by an 8 min digestion at 20 °C with a 1:1500 weight ratio of affinity-purified papain (*23*) and from $Pl^{st}$ and $Pl^{c}$ by a 10-min digestion at 15 °C with a 1:1000 w/w ratio in 20 mM MOPS, 60 mM NaCl, 2 mM $MgCl_2$, 0.1 mM $CaCl_2$, 0.1 mM EDTA, 3 mM $NaN_3$, and 0.5 mM DTT (*24*). The digestion was stopped with 100 $\mu$g/mL leupeptin. S1 was precipitated by addition of saturated ammonium sulfate to 55% saturation and redissolved in buffer containing 5−10 $\mu$g/mL leupeptin. After dialysis the S1 was clarified by centrifugation for 30 min at 40 000 rpm.

*Motility Assays.* Freshly prepared myosins in 0.6 M NaCl, 0.1 mM $CaCl_2$, 5 mM phosphate pH 7, 3 mM $NaN_3$, and 1 mM $MgCl_2$ were centrifuged at 100 000 rpm in a Beckman ultracentrifuge in the presence of ATP and actin to remove heads that cannot be dissociated from actin by ATP. Myosin dissolved in 0.3 M NaCl containing buffer was laid down on a nitrocellulose-coated coverslip to study the movement of monomeric myosins. Myosin filaments were formed by laying down the myosin in 0.15 M NaCl buffer. All assays were performed in 25 mM imidazole pH 7, 25 mM KCl, 4 mM $MgCl_2$, 1 mM EGTA, 1.1 mM $CaCl_2$, and 1 mM MgATP, in the presence of excess regulatory light chain at 25 °C. Actin filaments were visualized with rhodamine-labeled phalloidin (*25*). Photobleaching was reduced by 0.1 mg/mL glucose oxidase, 0.018 mg/mL catalase, and 2.3 mg/mL glucose (*26*). Actin filament detection and analysis was performed as previously described (*28*). The velocities of eight or more actin filaments were analyzed for each group, and values are expressed as means and their standard deviations.

Scheme 1

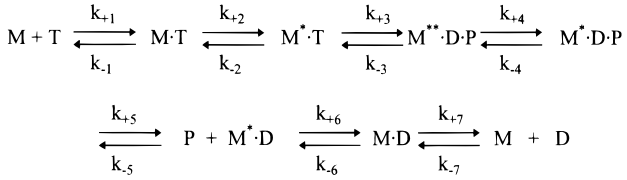


*Stopped-Flow Experiments.* Stopped-flow experiments were performed at 20 °C with a Hi-Tech Scientific SF61 or SF-61MX stopped-flow spectrophotometer equipped with a 100W Xe/Hg lamp and a monochromator. Pyrene fluorescence was excited at 365 nm and detected after passage through a KV 389-nm cutoff filter. Tryptophan fluorescence, excited at 290 nm, was monitored through a WG 320-nm cutoff filter. Light scattering was collected at 90° to the incident light at 405 nm. Data were stored and analyzed using software provided by Hi-Tech. Transients shown are the average of three to five consecutive shots of the stopped-flow machine. All concentrations refer to the concentration of the reactants after mixing in the stopped-flow observation cell. The experimental buffer used throughout was 20 mM MOPS, 5 mM $MgCl_2$, and 100 mM KCl, pH 7.0.

*Affinity of Actin for S1.* The affinities were measured using a novel stopped-flow method in which 30 nM phalloidin-stabilized pyr-actin was preincubated with different concentrations of S1. The complex was then mixed with ATP in the stopped-flow cell, and the amplitude of the observed transient gave an estimate of the concentration of the acto·S1 complex present at equilibrium (*27*).

*Transient Kinetic Analysis.* The ATP binding and hydrolysis by the scallop S1s have been analyzed in terms of the model shown in Scheme 1 based on that of Bagshaw et al. (*29*), where M is S1 and the asterisks refer to different conformations of the protein as detected by intrinsic protein fluorescence. Step 1 is the formation of the binary collision complex, followed by an almost irreversible rapid isomerization to the M*·ATP complex. This is followed by the reversible cleavage step. In a subsequent rate-limiting step phosphate is released, followed by a faster release of ADP. Both $P_i$ release and ADP release are two-step processes, consisting of an isomerization step followed by a dissociation step.

The experiments in the presence of actin were analyzed in terms of models developed by Millar and Geeves (*30*) and Siemankowski and White (*31*), in which A and M represent actin and S1, respectively. The first step after mixing acto·S1 and ATP is the rapid equilibration between A·M and ATP defined by the equilibrium constant $K_1$. This is followed by an isomerization of the ternary complex which limits the maximum rate of actin dissociation from the

[1] Abbreviations: $Pl^{st}$, *Placopecten* striated; $Pl^{c}$, *Placopecten* catch; $Ar^{st}$, *Argopecten* striated; $Rb^{st}$, rabbit striated; S1, subfragment 1; HMM, heavy meromyosin; pyr-actin, pyrene-labeled actin; mantADP, 2′(3′)-*O*-methylanthranilyladenosine 5′-diphosphate.

Scheme 2

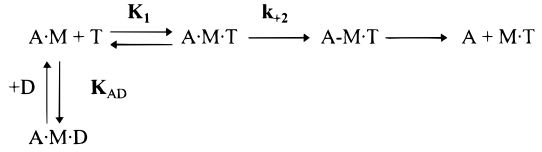


Scheme 3

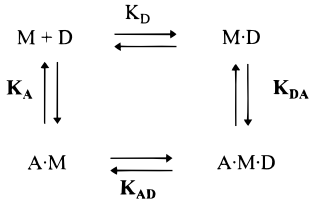


complex. Thus, the observed rate constant for the ATP-induced dissociation of actin from the complex is defined at low ATP concentrations by

$$k_{obs} = [ATP]\boldsymbol{K_1 k_{+2}} \quad (1)$$

Scheme 3 demonstrates the coupling between the actin and the nucleotide binding site. The presence of actin alters the affinity of ADP to S1 and vice versa. The affinity of S1 for ADP is given by $K_D$, and in terms of Scheme 1 $K_D$ is given by $1/K_6K_7$. The rate constant for ADP binding to S1 is defined by $k_{+D} = k_{-6}$, and the dissociation rate constant is given by $k_{-D} = k_{-6}/K_7$.

The affinity of S1 for actin is defined by $\boldsymbol{K_A}$. If ADP binds to the A·M complex, the affinity of actin for S1 is weakened and the ternary complex A·M·D is formed. The equilibrium constant for this process is $\boldsymbol{K_{DA}}$. Binding of actin to the S1·ADP complex alters the affinity of S1 for ADP, which also leads to the formation of the ternary complex A·M·D. The affinity of actin for M·D is defined by $\boldsymbol{K_{AD}}$.

## RESULTS

*Motility and Myosin ATPase*. Previous experiments have shown that the steady-state ATPase activities of the three myosin isoforms differ. It was of interest to see whether velocity of actin filament movement is also dependent on the particular myosin isoform. The movement of fluorescently labeled actin filaments over myosin molecules or filaments bound to nitrocellulose-coated coverslips was recorded by using a camera for several minutes. To reduce the effects of variability between different myosins in the measurements, the same myosin preparation was used for enzymatic activity and for motility (Table 1). The velocity of actin movement on both the filamentous and the monomeric forms of myosin was measured. The measurements were repeated on at least two separate myosin preparations from each of the three myosin isoforms. The rates of actin translocation on myosin monomers and on myosin filaments were very similar, and the data obtained by the use of the two forms were averaged. The results showed that $Pl^{st}$ muscle myosin moved actin faster (3.8 $\mu$m/s) than $Pl^{c}$ muscle myosin (0.85 $\mu$m/s) (Table 1). $Pl^{st}$ myosin also seemed to move a little faster than $Ar^{st}$ muscle myosin (2.6 $\mu$m/s).

These data are in very good agreement with previous measurements of the motility of $Ar^{st}$ and $Pl^{st}$ muscle myosins of 2.0 and 3.6 $\mu$m/s, respectively (*32*). The earlier data were obtained using a *Nitella*-based motility assay. The results of motility assays employing movement of actin filaments over a myosin surface and movement of myosin-coated beads over actin lattices are similar. The velocity of movement of these three scallop myosins seems to vary in the same direction as their steady-state ATPase activated by actin. $Pl^{st}$ myosin, with the highest steady-state ATPase activity, moves actin the fastest, and $Pl^{c}$ muscle myosin, with the lowest steady-state ATPase, moves actin the slowest. The values for $Ar^{st}$ myosin were intermediate both in motility and in ATPase activity (Table 1). It is noteworthy that the $V_{max}$ values of the S1s of the different myosins in the presence of actin show differences similar to those of the intact myosins.

*Protein Fluorescence Changes Associated with S1−ATP Interaction*. The addition of excess ATP to scallop S1 produced increases in intrinsic protein fluorescence of 13%, 10%, and 5% for $Ar^{st}$, $Pl^{st}$, and $Pl^{c}$, respectively, compared to a value of 20% for $Rb^{st}S1$. This signal was used to measure the rate of ATP binding and turnover in stopped-flow measurements. Figure 1A shows the fluorescence changes observed when 0.5 $\mu$M scallop S1 was mixed with 2 $\mu$M ATP. An exponential increase in fluorescence was seen, followed by a short steady state and then a decay of fluorescence back to the original value. The rise in fluorescence could be described by a single exponential, and the observed rate constant ($k_{obs}$) was linearly dependent on the ATP concentration in the range of 5−25 $\mu$M for all three S1s. The gradient of the plot in Figure 1B defines the rate constant of ATP binding ($K_1k_{+2}$), which is $5.1 \times 10^6$ $M^{-1}$ $s^{-1}$ for $Pl^{c}S1$ and 1/3 slower for $Pl^{st}S1$ and $Ar^{st}S1$ (see Table 2). At higher ATP concentrations the plot of $k_{obs}$ vs ATP concentration showed a deviation from linearity, and clear evidence of saturation of $k_{obs}$ was obtained for $Pl^{st}S1$. The data are shown in Figure 1C with a best fit to a hyperbola ($k_{obs} = k_{max}[ATP]/([ATP] + K_{0.5})$) superimposed. This gave an estimate of $k_{max}$ of around 500 $s^{-1}$ for $Pl^{st}S1$. For $Pl^{c}$ and $Ar^{st}S1$, although deviations from the linear fit were observed, no clear saturation of $k_{obs}$ was observed at ATP concentrations where $k_{obs} \approx 600$ $s^{-1}$ (Figure 1C). Therefore, it was not possible to make any realistic estimates for $k_{max}$. For RbS1 this maximal rate, $k_{max}$, has been shown to correspond to the rate of the ATP hydrolysis step ($k_{+3} + k_{-3}$). For RbS1 a fluorescence change is thought to occur on both the conformational change following the ATP binding and the subsequent hydrolysis step. One piece of evidence for this is that the amplitude of the fluorescence change decreases with high ATP concentrations. For the scallop S1s the observed fluorescence amplitude is smaller than that for RbS1, and after correction for any loss of amplitude in the dead time of the instrument, no loss of amplitude was observed at ATP concentrations up to 200 $\mu$M, which is consistent with a fluorescence change occurring only on the hydrolysis step. This is supported by the lack of any measurable protein fluorescence change on ADP binding to the S1s. In addition, the two Trps in the nucleotide binding pocket thought to be responsible for the fluorescence change in $Rb^{st}S1$ are absent in all three scallop S1s (similar to *Dictyostelium discoideum* myosin). W113 and W131 in the chicken sequence are replaced by G110 and R128 in the three scallops. Thus, $k_{max}$ for ATP binding to $Pl^{st}S1$ can be provisionally assigned to $k_{+3} + k_{-3}$.

Table 1: Motility and ATPase Activity of Myosins[a]

| | motility ($\mu$m/s) | ATPase − calcium ($\mu$mol min$^{-1}$ mg$^{-1}$) | ATPase + calcium ($\mu$mol min$^{-1}$ mg$^{-1}$) | sensitivity (%) |
|---|---|---|---|---|
| *Placopecten* striated | 3.80 ± 0.94 | 0.022 ± 0.024 | 1.320 ± 0.31 | 98 ± 1 |
| *Placopecten* catch | 0.85 ± 0.09 | 0.007 ± 0.001 | 0.122 ± 0.06 | 93 ± 4 |
| *Argopecten* striated | 2.62 ± 0.52 | 0.024 ± 0.003 | 0.334 ± 0.04 | 93 ± 2 |

[a] Motility data were obtained from measurements on 8−26 individual actin filaments using two or more independent myosin preparations for all three groups. All experiments were performed at 25 °C in the presence of excess regulatory light chains. Actin-activated ATPase activities of myosins used for motility assays were obtained in a pH stat at pH 7.6: 0.5−1 mg of myosin and 1 mg of actin in 10 mL of 2 mM MgATP, 20 mM NaCl, 1 mM $MgCl_2$, and 0.1 mM EGTA in the absence and the presence of 0.2 mM $CaCl_2$. Calcium sensitivity = (1 − ATPase$^{EGTA}$/ATPase$^{calcium}$) × 100.

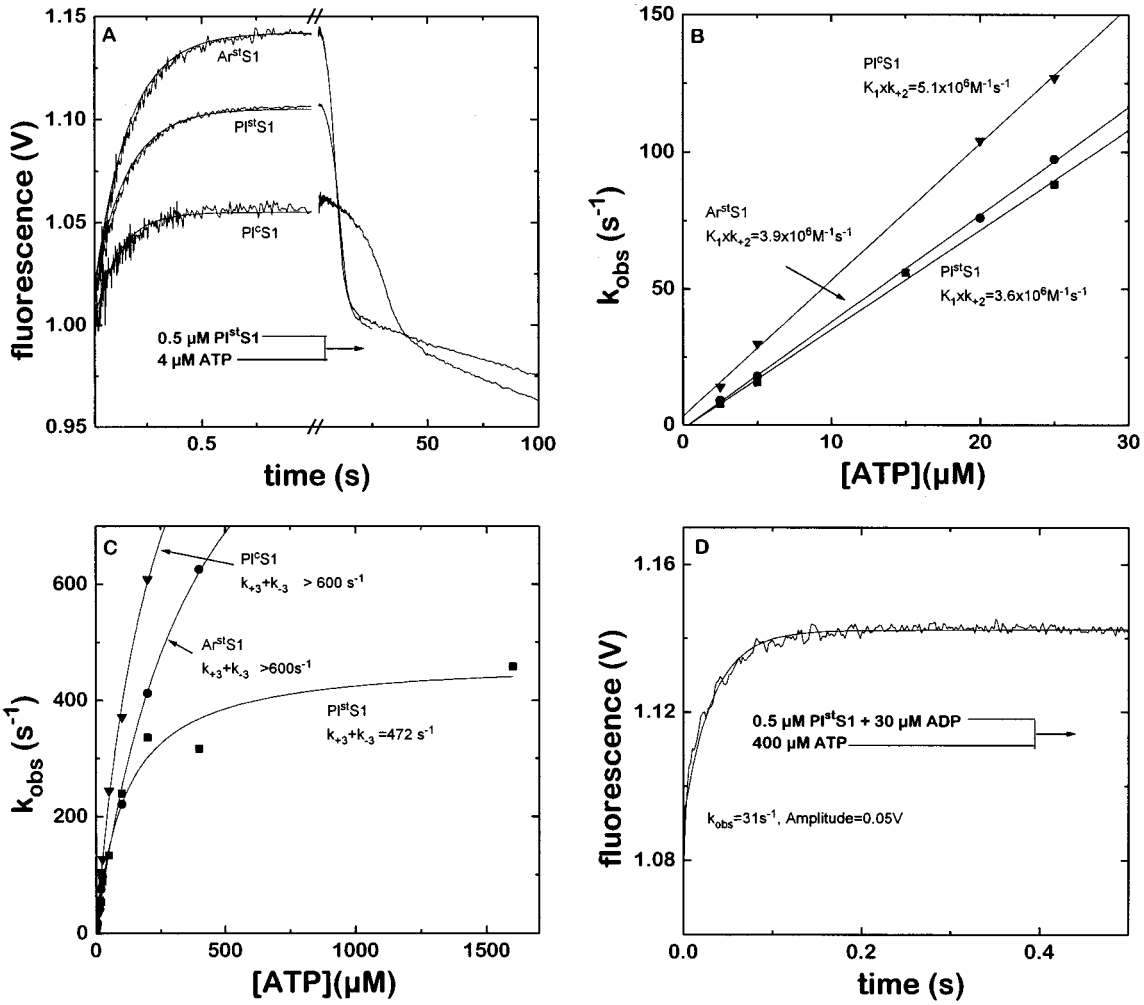


FIGURE 1: Interaction of nucleotide with scallop myosin S1. (A) Protein fluorescence change on 2 $\mu$M ATP binding to 0.5 $\mu$M S1 recorded in a stopped-flow apparatus. (B, C) Dependence of the observed rate constant of the fluorescence change on ATP concentration. Data in panel B were fitted to a straight line, with $K_1k_{+2}$ defined by the gradient, and data in panel C were fitted to a hyperbola with $k_{max} = k_{+3} + k_{-3}$. $K_{0.5}$ is 240 $\mu$M for Pl$^c$S1, 113 $\mu$M for Pl$^{st}$S1, and 390 $\mu$M for Ar$^{st}$S1. The other parameters are listed in Table 2. Symbols: Pl$^{st}$S1 (■), Pl$^c$S1 (▼), Ar$^{st}$S1 (●). (D) Rate of displacement of ADP from scallop S1. Stopped-flow record of the increase in intrinsic protein fluorescence during the binding of 400 $\mu$M ATP to 0.5 $\mu$M Pl$^{st}$S1, premixed with 30 $\mu$M ADP. The observed rate constant is 31 s$^{-1}$, and the amplitude of the fluorescence change is about 0.05 V. Conditions: 20 mM MOPS, 5 mM $MgCl_2$, and 100 mM KCl, pH 7.0, 20 °C.

If the ATP concentrations are limited to only a few-fold excess of the S1 concentration as shown in Figure 1A, the subsequent recovery of the protein fluorescence allows two estimates of the ATPase rate, one dependent on, and one independent of, S1 concentration. The return of fluorescence to the initial level is approximated by an exponential and defines the rate-limiting step of the ATP turnover normally assigned to $P_i$ release. This observed exponential was 0.16 s$^{-1}$ for Pl$^c$, 0.35 s$^{-1}$ for Pl$^{st}$, and 0.32 s$^{-1}$ for Ar$^{st}$S1 (Figure 1A) and was independent of the concentration of S1 used and of the ATP concentration, provided the $P_i$ and ADP dissociate totally from the S1. The other ATPase was estimated from the time between $t_1$, when the fluorescence increase was 50% complete, and $t_2$, when the decrease was 50% complete. The ATPase is given by [ATP]/($t_2$ − $t_1$), and $k_{cat}$ is the ATPase rate/[S1]. The resulting values are 0.16, 0.37, and 0.44 s$^{-1}$. The good correspondence between the two estimates provides an internal control for the quality of the protein preparation. Only the results for Ar$^{st}$S1 differ significantly. These data are in good agreement with those obtained in a steady-state assay (*7*).

Table 2: Results of the Transient Kinetic Analysis

| | rate constant | Rb$^{st}$S1 | Pl$^{st}$S1 | Pl$^{c}$S1 | Ar$^{st}$S1 |
|---|---|---|---|---|---|
| nucleotide binding to acto·S1 | $\boldsymbol{K_1k_{+2}}$ ($M^{-1}$ $s^{-1}$) | $2.1 \times 10^6$ | $1.6 \times 10^6$ | $2.8 \times 10^6$ | $2.5 \times 10^6$ |
| | $\boldsymbol{K_{AD}}$ ($\mu$M) | 200 | 670 | 76 | 480 |
| | $\boldsymbol{k_{-AD}}$ ($s^{-1}$) | | >400 | >200 | >200 |
| actin binding to S1 | $\boldsymbol{K_A}$ (nM) | 30 | 500 | 175 | 440 |
| | $\boldsymbol{k_{+A}}$ ($M^{-1}$ $s^{-1}$) | $3.9 \times 10^6$ | $6.2 \times 10^6$ | $6.2 \times 10^6$ | $7.9 \times 10^6$ |
| | $\boldsymbol{k_{-A}}$ ($s^{-1}$) | 0.11 | 2.5 | 4.5 | 3.1 |
| nucleotide binding to S1 (ATP) | $K_1k_{+2}$ ($M^{-1}$ $s^{-1}$) | $2.3 \times 10^6$ | $3.6 \times 10^6$ | $5.1 \times 10^6$ | $3.9 \times 10^6$ |
| | $k_{+3}+k_{-3}$ ($s^{-1}$) | 130 | 470 | (>600) | |
| mantATP | $K_1k_{+2}$ ($M^{-1}$ $s^{-1}$) | $3.2 \times 10^6$ | $5.1 \times 10^6$ | $6.8 \times 10^6$ | $5.9 \times 10^6$ |
| mantADP | $k_{-D}$ ($s^{-1}$) | 0.22 | 25 | 28 | 17 |
| | $k_{+D}$ ($M^{-1}$ $s^{-1}$) | $2.1 \times 10^6$ | $2.1 \times 10^6$ | $3.1 \times 10^6$ | $1.5 \times 10^6$ |
| | $K_D$ (calc) ($\mu$M) | 0.1 | 12 | 9 | 11 |
| ADP | $K_D$ ($\mu$M) | 1 | 4.5 | 2.5 | 9.8 |
| | $k_{-D}$ ($s^{-1}$) | 2.3 | 35 | 32 | 18.5 |

*Interaction of ADP and Mant Nucleotides with Scallop S1*. As stated above, the binding of ADP to scallop S1 did not produce any measurable increase in protein fluorescence. However, the rate of binding of 100 $\mu$M ATP to S1 was reduced when either S1 or ATP was premixed with ADP, suggesting that ADP does compete with ATP in binding to S1.

The ADP dissociation rate constant was determined for all three S1s by displacing ADP from S1 by a large excess of ATP (1 $\mu$M S1 and 30 $\mu$M ADP were mixed with 400 $\mu$M ATP) and measuring the increase of protein fluorescence as ATP binds (Figure 1D). This gave $k_{-D}$ values of 31 $s^{-1}$ for Pl$^{st}$S1, 32 $s^{-1}$ for Pl$^{c}$S1, and 18.5 $s^{-1}$ for Ar$^{st}$S1. S1, 0.5 $\mu$M, was mixed with different amounts of mantATP, and the observed mant fluorescence increase was described by a single exponential (data not shown). The observed rate constants were linearly dependent on the mantATP concentration over the range of 2.5−20 $\mu$M. The second-order binding constants ($K_1k_{+2}$) obtained from the slope are listed in Table 2. The binding of mantATP is 30−40% faster than that of ATP for all 3 S1s. The amplitudes of the fluorescence increases were about 220% for Pl$^{st}$S1, 100% for Pl$^{c}$S1, and 190% for Ar$^{st}$S1 compared to 160% for RbS1.

The binding of mantADP to the scallop S1s was also followed over a similar range of concentrations. The second-order rate constants are shown in Table 2. The fluorescence changes observed on mixing 5 $\mu$M mantADP with 1 $\mu$M S1 were 60% for Pl$^{st}$S1, 50% for Pl$^{c}$S1, and 65% for Ar$^{st}$S1. The rate of dissociation of mantADP from the S1s ($k_{-D}$) was measured by displacement of 50 $\mu$M nucleotide analogue from a 0.5 or 1 $\mu$M scallop S1·mantADP complex by 100, 200, and 300 $\mu$M ATP. The observed rate constant for the reaction was independent of the ATP concentrations used, with $k_{-D}$ values of 25, 28, and 17 $s^{-1}$ for Pl$^{st}$, Pl$^{c}$, and Ar$^{st}$-S1. The ratio of the two measurements, $k_{-D}/k_{+D}$ (= $K_D$ for mantADP) gives values of 12 and 9 $\mu$M for the two PlacoS1s and 11 $\mu$M for Ar$^{st}$S1. These $K_D$'s are similar to those for ADP without the fluorescent label (see below).

*Interaction of S1 with Actin and Nucleotides. (A) ATP-Induced Dissociation of Acto·S1*. pyr-actin·S1, 0.25 $\mu$M, was mixed with different amounts of ATP, and the exponential increase in pyrene fluorescence as the complex dissociated was observed. Figure 2A shows a typical stopped-flow trace for 5 $\mu$M ATP mixed with 0.25 $\mu$M acto·Pl$^{st}$S1. All traces could be fitted to a single exponential. The observed rate constants were linearly dependent upon the ATP concentrations in the range of 5−20 $\mu$M (Figure 2B). The second-order binding constants ($\boldsymbol{K_1k_{+2}}$) are defined by the gradi-

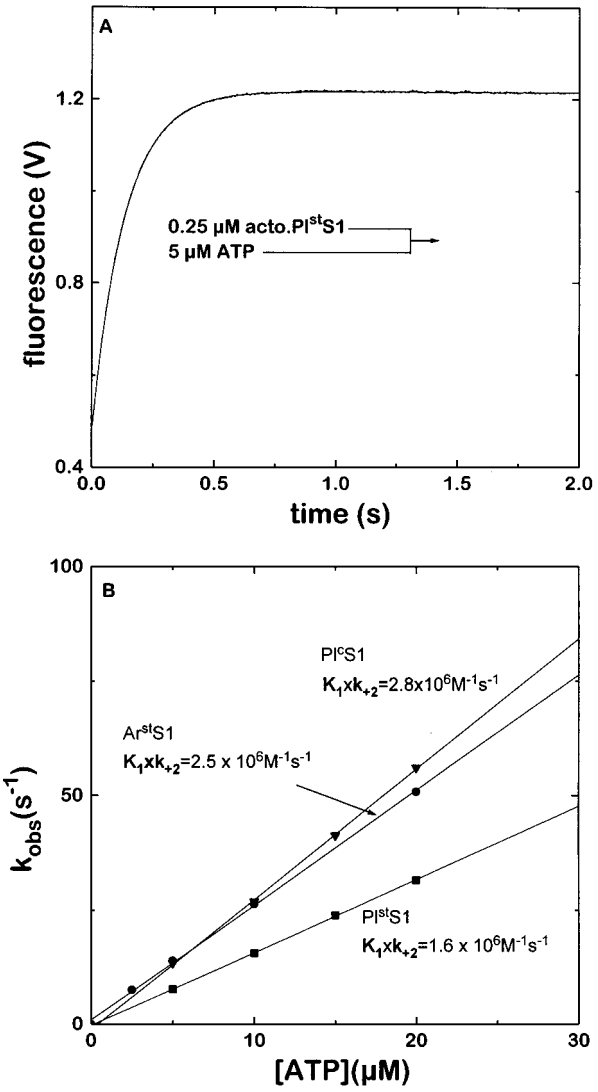


FIGURE 2: ATP-induced dissociation of pyr-acto·S1 complexes. (A) Increase in pyrene fluorescence recorded during the dissociation of 0.25 $\mu$M pyr-acto·Pl$^{st}$S1 induced by 5 $\mu$M ATP. A single exponential with $k_{obs}$ = 7.4 $s^{-1}$ and an amplitude of the fluorescence change of 0.75 V is superimposed. (B) Plot of $k_{obs}$ vs [ATP]. The observed rate constant is linearly dependent on ATP concentration in the range of 5−20 $\mu$M. The slopes correspond to $\boldsymbol{K_1k_{+2}}$. The values of $\boldsymbol{K_1k_{+2}}$ are given in Table 2. Symbols: Pl$^{st}$S1 (■), Pl$^{c}$S1 (▼), Ar$^{st}$S1 (●). Conditions: see Figure 1.

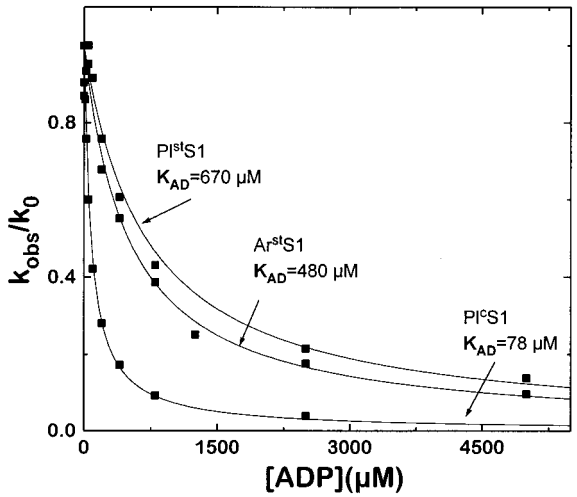


FIGURE 3: ADP inhibition of ATP-induced dissociation of pyr-acto·S1 complexes. Plot of $k_{obs}/k_o$ vs ADP concentration. The dissociation constants of the ADP complexes were determined by fitting a plot according to the following equation: $k_{obs}/k_o = 1/(1 + [ADP]/\boldsymbol{K_{AD}})$; $k_o$ = observed rate constant in the absence of ADP. The data are listed in Table 2. Conditions: see Figure 1.

ent: $2.8 \times 10^6$ $M^{-1}$ $s^{-1}$ for Pl$^c$S1, a similar value for Ar$^{st}$S1, and a factor of 2 slower for Pl$^{st}$S1 (see Table 2). Although some deviations from a straight-line fit were seen, there was little evidence of saturation of $k_{obs}$ up to a rate of 800 $s^{-1}$. Fitting a hyperbola to the data predicts a maximum rate constant of about 2000 $s^{-1}$ for all three proteins, but the error on these estimates is very large.

*(B) ADP Inhibition of ATP-Induced Dissociation of acto·S1*. To measure the ADP affinity for acto·S1, 0.25 $\mu$M pyr-acto·S1 was mixed with 100 $\mu$M ATP in the presence of different amounts of ADP and we measured the rate of the ATP-induced dissociation reaction. The fluorescence increase could again be fitted with a single exponential. A plot of the observed rate constants for this reaction against the ADP concentration can be fitted to

$$k_{obs}/k_o = 1/(1 + ([ADP]/\boldsymbol{K_{AD}})) \qquad (2)$$

with $k_o$ = observed rate constant in the absence of ADP, which gave $\boldsymbol{K_{AD}}$ values for ADP binding of 670 $\mu$M for Pl$^{st}$S1, 480 $\mu$M for Ar$^{st}$S1, and about 78 $\mu$M for Pl$^c$S1 (Figure 3). This means that acto·Pl$^{st}$S1 and acto·Ar$^{st}$S1 have an almost 5−10 times weaker affinity for ADP than acto·Pl$^c$S1. This analysis assumes that the ADP is in rapid equilibrium with acto·S1. To check this assumption, we attempted to define the ADP dissociation rate constant. However, because the affinities of both actin and ADP to S1 in the ternary complex are weak, it is not possible to form a stable acto·S1·ADP complex. We therefore measured the rate of dissociation of acto·S1 by ATP when the ATP is mixed with ADP at a concentration 3 times the estimated $\boldsymbol{K_{AD}}$. In each case the $k_{obs}$ was one-fourth of that in the absence of ADP (as predicted by eq 2). In addition, $k_{obs}$ was linearly dependent upon ATP concentration until the observed rate constant was in excess of 200 $s^{-1}$. Thus, ADP is competing with ATP binding and the ADP release rate constant, $\boldsymbol{k_{-AD}}$, is in excess of 200 $s^{-1}$. Therefore, the conditions for rapid equilibrium are at least approximately met.

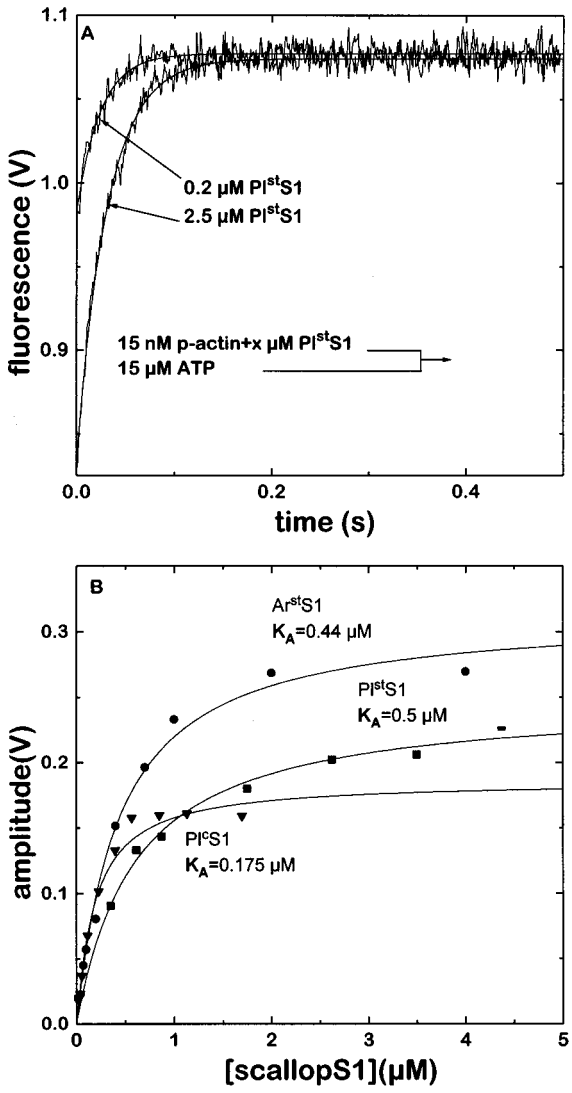


FIGURE 4: Determination of the affinity of scallop S1s for pyr-actin by measuring the amplitude of the pyr-acto·S1 dissociation reaction. (A) Stopped-flow records of the dissociation of 15 nM pyr-actin from 0.2 and 2.5 $\mu$M Pl$^{st}$S1 induced by 15 $\mu$M ATP. The amplitudes of the fluorescence change are 0.09 and 0.24 V for 0.2 and 2.5 $\mu$M Pl$^{st}$S1, respectively. (B) Plot of the amplitudes against S1 concentration. The data were fitted to binding isotherms. The fitted parameters are listed in Table 2 ($\boldsymbol{K_A}$). Symbols: Pl$^{st}$S1 (■), Pl$^c$S1 (▼), Ar$^{st}$S1 (●). Conditions: see Figure 1.

*(C) Equilibrium Actin Binding to S1*. We measured the affinity of actin for Pl$^{st}$S1 as described (*27*) in Phalloidin-stabilized pyr-actin, 15 nM, was mixed with different amounts of S1, and the fluorescence increase during the dissociation of the complex with ATP (Figure 4A) was measured. The amplitudes of the reactions (which are proportional to the amount of acto·S1 complex formed) were plotted against the S1 concentration before mixing (Figure 4B). Pl$^{st}$S1 behaves like Ar$^{st}$S1, and a $\boldsymbol{K_A}$ of around 500 nM could be measured (Figure 4B), whereas the $K_A$ for Pl$^c$-S1 (175 nM) was 3-fold tighter. At 10 mM KCl the $K_A$ for Pl$^c$S1 binding to actin was around 30 nM, suggesting that the overall salt dependence of the $\boldsymbol{K_A}$ is similar to that of Rb$^{st}$S1 (*27*).

*(D) Actin Binding and Dissociation*. The rate of actin binding to S1 was measured by mixing excess pyr-actin with 0.5 $\mu$M S1 and monitoring the decrease of pyrene fluorescence as actin binds (Figure 5A). The observed rate

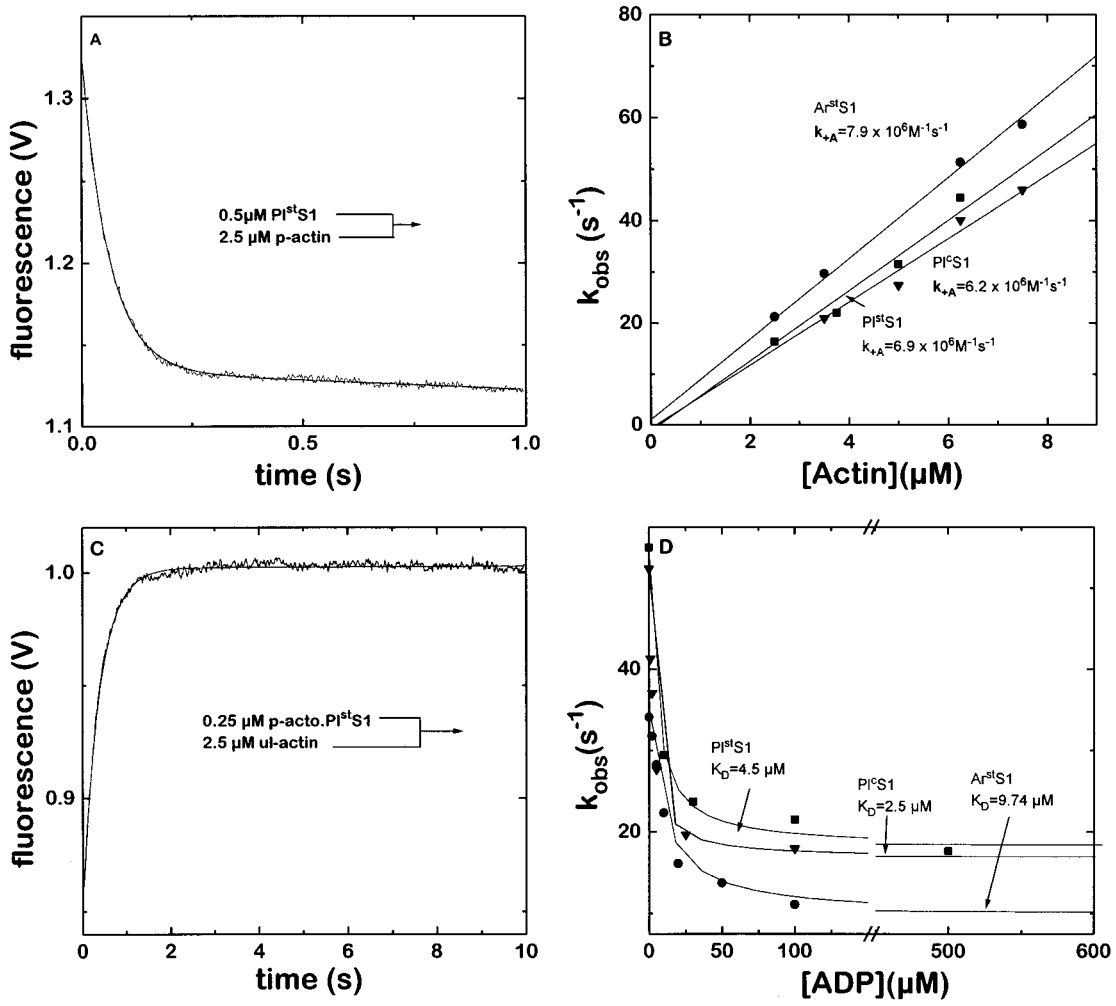


FIGURE 5: Binding of pyr-actin to scallop myosin S1. (A) Stopped-flow record of the change of pyrene fluorescence during the binding of 2.5 $\mu$M pyr-actin to 0.5 $\mu$M Pl$^{st}$S1 with an observed rate constant of 16 $s^{-1}$ and an amplitude of the fluorescence change of about 0.2 V. (B) Dependence of the observed rate constant on actin concentrations of 2.5−7.5 $\mu$M. The data are fitted to straight lines, with $\boldsymbol{k}_{+\mathbf{A}}$ given by the slopes. (C) Stopped-flow trace of the increase in pyrene fluorescence during the replacement of the pyr-actin of the pyr-acto·Pl$^{st}$S1 complex with 2.5 $\mu$M actin. A single-exponential fit with $k_{obs}$ = 2.5 $s^{-1}$ and an amplitude of 0.15 V is superimposed. The observed rate constant is the "off " rate for actin ($k_{-A}$). All the resulting values are summarized in Table 2. (D) Reduction of the rate of 8 $\mu$M pyr-actin binding to S1 in the presence of ADP. Plot of $k_{obs}$ vs ADP concentration. The dissociation constants of the scallop S1 ADP complexes were determined by fitting the plot according to the equation

$$k_{obs} = \boldsymbol{k}_{+A}\frac{K_D}{K_D + [ADP]} + \boldsymbol{k}_{+DA}\frac{[ADP]}{K_D + [ADP]}$$

where $\boldsymbol{k}_{+\mathbf{A}}$ = observed rate constant in the absence of ADP, and $\boldsymbol{k}_{+\mathbf{DA}}$ = rate constant in the presence of saturating ADP concentrations. Symbols: Pl$^{st}$S1 (■), Pl$^{c}$S1 (▼), Ar$^{st}$S1 (●). Conditions: see Figure 1.

constants were linearly dependent on the actin concentration up to 8 $\mu$M (Figure 5B). The second-order binding rates given by the slope are 6.2 × $10^6$ $M^{-1}$ $s^{-1}$ for Pl$^{st}$S1 and Pl$^{c}$S1 and 7.9 × $10^6$ $M^{-1}$ $s^{-1}$ for Ar$^{st}$S1. All scallop S1s bind actin twice as fast as Rb$^{st}$S1. The dissociation rate constant for actin was measured by displacing 0.25 $\mu$M pyr-actin from the acto·S1 complex by a 10-fold excess of unlabeled actin. The single-exponential increase of pyrene fluorescence during the displacement could be measured. The dissociation rate is given by the observed rate constant. It is 2.8 $s^{-1}$ for Pl$^{st}$S1 and Ar$^{st}$S1 and 2-fold faster for Pl$^{c}$S1 (Figure 5C). The rate of Rb$^{st}$S1 binding to actin is reduced approximately 20-fold when ADP is bound to S1. If this is also true for the scallop proteins, the reduction in the $k_{obs}$ for S1 binding to excess actin can be used to measure the extent of saturation of S1 with ADP. Different amounts of ADP were premixed with 0.5 $\mu$M Pl$^{st}$S1, and the decrease in pyrene fluorescence was recorded during the binding of pyr-actin (data not shown). If S1 exists in an equilibrium mixture of S1 and S1·ADP, the observed fluorescence change on mixing with excess actin is dependent upon the relative rates of ADP binding to S1 and actin binding to S1 and S1·ADP. If $[ADP]k_{+D} + k_{-D} \gg [A]\boldsymbol{k}_{+\mathbf{A}}$ and $[A]\boldsymbol{k}_{+\mathbf{DA}}$, the resulting equation is

$$k_{obs} = \boldsymbol{k}_{+A}\frac{K_D}{K_D + [ADP]} + \boldsymbol{k}_{+DA}\frac{[ADP]}{K_D + [ADP]} \quad (3)$$

where $k_{+A}$ and $k_{+DA}$ are the rate constants for S1 and S1·ADP binding to actin and $K_D$ is the affinity of ADP for S1. If $[ADP]k_{+D} + k_{-D} \ll [A](\boldsymbol{k}_{+\mathbf{A}} + \boldsymbol{k}_{+\mathbf{DA}})$, two phases will be seen with $k_{obs}$ values of $\boldsymbol{k}_{+\mathbf{A}}[A]$ and $\boldsymbol{k}_{+\mathbf{DA}}[A]$. Because only one phase was observed, compatible with a fast equilibrium between S1 and S1·ADP, the observed rate constant was

plotted against the ADP concentration. The dependence of $k_{obs}$ on ADP was fitted to eq 3. This analysis (Figure 5D) gave $K_D$ values for ADP binding to Pl$^{st}$S1 of 4.5 $\mu$M, to Pl$^{c}$S1 of 2.5 $\mu$M, and to Ar$^{st}$S1 of 9.8 $\mu$M.

## DISCUSSION

In this study we have analyzed the rates of the individual steps of the ATPase cycles of three S1 isoforms obtained from the regulated myosins of *Placopecten* catch and striated and *Argopecten* striated adductor muscles. Although the sequences of the heavy chains of the two Placo S1s are almost identical, the S1 ATPase (Figure 1A) and the $V_{max}$ (*7*) differ considerably between them. The two striated S1s differ by less than a factor of 2. Hybrid studies have established that differences in the ATPase activity arise from variations in the heavy chain (*7*). Since the PlS1s differ in the sequence of the heavy chain that encodes surface loop 1 (residues 200−214) while the sequences of surface loop 2 (residues 625−646) are identical, our overall goal was to correlate this sequence variability near the nucleotide binding site with the individual rate constants of the ATPase cycle. We have also compared the constants obtained to those of S1s of the unregulated rabbit myosin and measured the motilities of the three scallop myosins because this functional parameter has been shown to be closely correlated with ADP release.

Since the three scallop S1s hydrolyze ATP by the same mechanism as all the other myosins so far studied, the mechanism shown in Schemes 1−3 can be applied.

The two striated S1s behave very similarly. None of the measured parameters differ by more than a factor of 2. The agreement between most of the constants, including the affinity of ADP for acto·S1, is even better (Table 2). The $V_{max}$ of the S1 ATPase and the actin velocities also differ by less than 2-fold. This indicates that the sequence variation between these two S1s may have little functional significance.

The comparison of the two scallop striated S1s with fast rabbit S1 shows interesting differences. The affinity of the scallop proteins for rabbit actin is 10-fold weaker than the affinity of rabbit S1 resulting from their higher dissociation rate constants. It is noteworthy that scallop actin is a $\beta$-actin, and the differences in part may be due to the small differences in the sequences of α- and $\beta$-actins. Nevertheless, $K_M$'s for the actin activation of the ATPases were similar to those of rabbit S1 at low ionic strength (*7*). The affinity of the scallop S1s for ADP and mantADP was considerably lower than the affinity of rabbit S1 mostly due to the higher dissociation rate constants from the scallop proteins. This property does not show a great variation between different mammalian and avian myosin S1s, but a similar low affinity was reported for the S1 of *Dictyostelium* cytoplasmic myosin II (*33*).

The maximum rate constant for the fluorescence change on ATP binding has been assigned to the rate of the ATP hydrolysis step, as for other myosins. This need not be correct, particularly as this event did not clearly reach saturation in the case of scallop S1s. Nevertheless, this fluorescence change accompanies only ATP binding and is not present upon ADP binding. The rate constants for mantATP and mantADP binding were similar to the rate constant for ATP binding. Therefore, the observed process could be a protein conformational change which precedes ATP hydrolysis rather than ATP hydrolysis itself.

Jackson and Bagshaw (*34*) completed a transient kinetic study of the $Ca^{2+}$-regulated Ar$^{st}$HMM in the absence of actin at lower ionic strength and higher pH (20 mM NaCl, pH 7.5). In general, the results presented here are in broad agreement with those of the HMM in the presence of $Ca^{2+}$. The rates of ATP and ADP binding and turnover are similar, as is the rate constant for ADP release from S1. Significantly, Jackson and Bagshaw were able to measure a maximum rate for the protein fluorescence change on ATP binding of 200 $s^{-1}$ (*34*). Whether this slower rate is due to the differences in conditions or due to a difference between HMM and S1 remains to be determined.

The affinity of ADP for the catch acto·S1 is 8−9-fold greater than the affinity of ADP for the two striated acto·S1s. This tighter ADP binding to the catch acto·S1 is the single major difference between the catch and striated preparations. The observation that there are very few differences between Ar$^{st}$ and Pl$^{st}$ S1s is a good internal control for this finding. The rest of the parameters measured for Pl$^{c}$S1 were similar to those of both Pl$^{st}$ and Ar$^{st}$ S1s. The rate of ATP-induced dissociation ($\boldsymbol{K_1k_{+2}}$) of acto·S1, the rates of ATP and ADP binding to S1, and the rates of ADP dissociation for S1 agreed within a factor of 2 between the catch and striated S1s. ADP release from acto·S1 was in each case too fast to measure (>200 $s^{-1}$). It is significant that the affinity of S1 for ADP does not change, while the affinity for acto·S1 is more than 8−9-fold weaker for Pl$^{st}$S1. This suggests that it is not the recognition of ADP by the S1 which has been altered but the ability of actin to displace the ADP.

The net rate of ADP release and ATP binding has been proposed to be the one that limits the overall speed of shortening of mammalian and avian muscles (*10*). It is of interest, therefore, that the equilibrium constant of ADP binding is the only one which appears significantly different in Pl$^{c}$S1, apparently influenced by the different sequence of surface loop 1. An important observation is that both the motility data presented here and the $V_{max}$ of the actin-activated ATPase (*7*) of the two PlS1s appear altered in a similar manner (3−4-fold), and this is associated with changes in ADP affinity for acto·S1.

Differences in the ATPase activity were also seen between catch and striated S1s in the absence of actin. Differences in steady-state S1-ATPases can result from errors in the concentration of active protein; however, the data presented here (Figure 1A) provide estimates of the rate of the limiting event in the ATPase cycle which are independent of the protein concentration. These differences lie between the proteins themselves, which suggests that changes in loop 1 affect the $P_i$ release step of the S1-ATPase in addition to the affinity of ADP for acto·S1. Thus the influence of loop 1 may be more far reaching than previously proposed (*11*).

An understanding of the role of ADP affinity (or ADP release) in contracting fibers requires the knowledge of ADP concentration in the cell, which is changing during contraction. However, the same problem is not a factor in the motility experiments where the free nucleotide concentration can be controlled and remains essentially constant due to the relatively large volume of the medium. Motility studies indicate a 3−4-fold difference in speed between Pl$^{st}$ and Pl$^{c}$.

The minimum allowable rate constant ($k_{min}$) and therefore the maximum lifetime of the attached state can be estimated from the unloaded shortening velocity ($V$) and the distance over which a cross-bridge can remain attached (*31*):

$$k_{min} = V/d$$

The values of $k_{min}$ can be estimated for Pl$^c$ and Pl$^{st}$ myosin. The measured motility speeds are 0.85 and 3.8 $\mu$m/s, respectively, and assuming a 10-nm attached distance, the lifetimes of the attached state will be as follows:

$$k_{min}(\text{Pl}^c \text{ myosin}) = 0.85/0.01 = 85 \text{ s}^{-1}$$

$$k_{min}(\text{Pl}^{st} \text{ myosin}) = 3.8/0.01 = 380 \text{ s}^{-1}$$

The rate of the limiting reactions cannot be slower than $k_{min}$. The minimum rate is in the range of $\boldsymbol{k}_{-\mathbf{AD}}$ for Pl$^{st}$ myosin (>200 s$^{-1}$). This means, as previous measurements have shown, that ADP dissociation can limit the unloaded shortening velocity. On the other hand, $k_{min}$ for Pl$^c$ myosin is considerably smaller than the estimated $\boldsymbol{k}_{-\mathbf{AD}}$ (>200 s$^{-1}$). Therefore, for catch S1, the step limiting velocity may be different.

Three different structural methods (*35*−*37*) have shown a structural change in mammalian smooth muscle S1 in response to ADP binding to the acto·S1 complex. Yet no structural change was observed with skeletal muscle acto·S1. Low-angle X-ray scattering studies with Ar$^{st}$S1 have shown only a very small structural change in the presence of millimolar ADP (K. Poole, personal communication). It would be of interest to know if the catch muscle S1 did show the larger structural change observed with smooth muscle S1, as this acto·S1 has the higher affinity for ADP associated with smooth muscle S1.

The role of the surface loops in relating unloaded contraction speed to ATPase activity in different muscles has been pointed out by Spudich (*11*). The two functions may be separately influenced by the two surface loops. In some studies, surface loop 1 modulates the actin-activated ATPase and surface loop 2 regulates actin motility. In molluscan myosins surface loop 1 can modulate both of these processes. We speculate that loop 1 in myosin can modulate ATPase activity as well as actin movement in motility assays because of changes in the ADP affinity of acto·S1. It could also introduce a different rate-limiting step which may be related to the ADP-induced structural changes seen in some acto·S1s.

## ACKNOWLEDGMENT

We thank Dr. Susan Lowey for the use of equipment for the fluorescence measurements, Rita Purcell for her help with manuscript preparation, and Nancy Adamek for the preparation of the rabbit proteins.

## REFERENCES

1. Cornelius, F. (1982) *J. Gen. Physiol. 70*, 821−834.
2. Castellani, L., and Cohen, C. (1987) *Science 235*, 334−337.
3. Takahashi, M., Sohma, H., and Morita, F. (1988) *J. Biochem. 104*, 102−107.
4. Achazi, R. K. (1979) *Pflue Arch. 379*, 197−201.
5. Cooley, L. B., Johnson, W. H., and Krause, S. (1979) *J. Biol. Chem. 254*, 2195−2198.
6. Rüegg, J. C. (1992) *Calcium in Muscle Contraction*, 2nd ed., Springer-Verlag, Berlin.
7. Perreault-Micale, C. L., Kalabokis, V. N., Nyitray, L., and Szent-Györgyi, A. G. (1996) *J. Muscle Res. Cell Motil. 17*, 543−553.
8. Perreault, C. L., Trybus, K. M., Geeves, M. A., Kurzawa, S., and Szent-Györgyi, A. G. (1997) *Biophys. J. 72*, A180.
9. Bárány, M. (1967) *J. Gen. Physiol. 50* (Suppl.), 197−218.
10. Siemankowski, R. F., Wiseman, M. O., and White, H. D. (1985) *Proc. Natl. Acad. Sci. U.S.A. 82*, 658−662.
11. Spudich, J. A. (1994) *Nature 372*, 515−518.
12. Uyeda, T. Q. P., Ruppel, K. M., and Spudich, J. A. (1994) *Nature 368*, 567−569.
13. Bobkov, A. A., Bobkova, E. A., and Reisler, E. (1996) *Proc. Natl. Acad. Sci. U.S.A. 93*, 2285−2289.
14. Kelley, C. A., Takahashi, M., Yu, J. H., and Adelstein, R. S. (1993) *Proc. Natl. Acad. Sci. U.S.A. 268*,12848−12854.
15. Sweeney, H. L., Faust, L., Brown, J. E., Milligan, R. A., Sellers, J. R., and Stein, L. A. (1996) *Biophys. J. 70*, A149.
16. Rovner, A. S., Freyson, Y., and Trybus, K. M. (1996) *J. Muscle Res. Cell Motil. 18*, 103−110.
17. Nyitray, L., Jancso, A., Ochiai, Y., Gráf, L., and Szent-Györgyi, A. G. (1994) *Proc. Natl. Acad. Sci. U.S.A. 91*, 12686−12690.
18. Lehrer, S. S., and Kewar, G. (1972) *Biochemistry 11*, 1211−1217.
19. Criddle, A. H., Geeves, M. A., and Jeffries, T. A. (1985) *Biochem. J. 232*, 343−349.
20. Hiratsuka, T. (1983) *Biochim. Biophys. Acta 742*, 496−508.
21. Woodward, S. K. E., Eccleston, J. F., and Geeves, M. A. (1991) *Biochemistry 30*, 422−430.
22. Stafford, W. F., Szentkiralyi, E. M., and Szent-Györgyi, A. G. (1979) *Biochemistry 24*, 5273−5280.
23. Funk, M. O., Nakagawa, Y., Skochdopole, J., and Kaiser, E. T. (1979) *Int. J. Pept. Protein Res. 13*, 296−303.
24. Kalabokis, V. N., and Szent-Györgyi, A. G. (1997) *Biochemistry* (in press).
25. Kron, S. J., and Spudich, J. A. (1986) *Proc. Natl. Acad. Sci. U.S.A. 83*, 6272−6276.
26. Kishino, A., and Yanagida, T. (1988) *Nature 334*, 74−76.
27. Kurzawa, S. E., and Geeves, M. A. (1996) *J. Muscle Res. Cell Motil. 17*, 669−679.
28. Warshaw, D. M., Desrosiers, J. M., Work, S. S., and Trybus, K. M. (1990) *J. Cell Biol. 111*, 453−463.
29. Bagshaw, C. R., and Trentham, D. R. (1974) *Biochem. J. 141*, 331−349.
30. Millar, N. C., and Geeves, M. A. (1983) *FEBS Lett. 160*, 141−148.
31. Siemankowski, R. F., and White, H. D. (1984) *J. Biol. Chem. 259*, 5045−5053.
32. Vale, R. D., Szent-Györgyi, A. G., and Sheetz, M. P. (1984) *Proc. Natl. Acad. Sci. U.S.A. 81*, 6775−6778.
33. Kurzawa, S. E., Manstein, D. J., and Geeves, M. A. (1997) *Biochemistry 36*, 317−323.
34. Jackson, A. P., and Bagshaw, C. R. (1988) *Biochem. J. 251*, 527−540.
35. Poole, K. J. V., Lorenz, M., Ellison, P., Evans, G., Rosenbaum, G., Boeseke, P., Holmes, K. C., and Cremo, C. R. (1997) *J. Muscle Res. Cell Motil. 18*, 264.
36. Whittaker, M., Wilson-Kubalek, E. M., Smith, J. E., Faust, L., Milligan, R. A., and Sweeney, H. L. (1995) *Nature 378*, 748−751.
37. Gollup, J., Cremo, C. R., and Cooke, R. (1996) *Nat. Struct. Biol. 3*, 796−802.

BI972844+